Chapter 34

Reaction Mechanisms of Pair Transfer

Ian J. Thompson

Lawrence Livermore National Laboratory,
PO Box 808, L-414, Livermore, CA 94551, USA
I-Thompson@llnl.gov

The mechanisms of nuclear transfer reactions are described for the transfer of two nucleons from one nucleus to another. Two-nucleon overlap functions are defined in various coordinate systems, and their transformation coefficients given between coordinate systems. Post and prior couplings are defined for sequential transfer mechanisms, and it is demonstrated that the combination of 'prior-post' couplings avoids non-orthogonality terms, but does not avoid couplings that do not have good zero-range approximations. The simultaneous and sequential mechanisms are demonstrated for the $^{124}\text{Sn}(\text{p},\text{t})^{122}\text{Sn}$ reaction at 25 MeV using shell-model overlap functions. The interference between the various simultaneous and sequential amplitudes is shown.

1. Introduction

Much of the evidence for nucleonic pairing in nuclei comes from energy expectation values, but important further information comes from the *transfer* of pairs of nucleons to or from another nucleus of known structure. In this regard, a more fundamental understating of nuclear reactions has been, and will continue to be (especially in the FRIB era), crucial to the nuclear physics community. This chapter focuses on the theory, calculation and model results for the reactions mechanisms of pair transfer.

Here we consider the reaction mechanisms for pair transfer between two nuclei, namely reactions that we can describe as $A(B+2, B)A+2$. Here, the two nucleons may be two neutrons, two protons, or a proton and a neutron, and are transferred from core B to core A. The nucleons may transfer either in one *simultaneous* step, or one after the other *sequentially*. If a distinguishable proton and a neutron are transferred, then both proton-then-neutron and neutron-then-proton routes need to be considered. Furthermore, these sequential and simultaneous routes contribute amplitudes that all add together *coherently*. This feature enables us to probe the nature of coherent two-nucleon superpositions in nuclei. Conversely, these superpositions, coupling orders and phase conventions have all to be defined consistently in a good calculation.

Subsequent sections will therefore consider the definition of two-nucleon overlap functions, their coordinate transformations, the definition of transfer matrix elements along with zero-range approximations and non-orthogonality corrections. Finally, some results are shown to illustrate the coherence effects in the reaction mechanisms of pair transfers.

In the last 50 years, a significant number of papers have been presented in which absolute differential cross sections have been calculated, and compared with experimental results.[1–19] Traditionally, for example in Ref. 9, the theory predictions have fallen well below the experimental data. This ratio has been called the 'unhappiness factor',[20,21] and has sometimes been more than 100. Most previous calculations modeled the transfer of a dineutron as a single cluster. And only from Charlton[8] were sequential transfer contributions considered. We find that modern calculations, such as as those of Potel *et al*,[19] are in considerably better agreement with experiment.

2. Bound States and Vertex Functions

The general theory of nucleon pair bound states defines the overlap function $\phi_I^J(\mathbf{r}, \boldsymbol{\rho}) = \langle \Phi_A(I) | \Phi_{A+2}(J) \rangle$ in terms of the Jacobi coordinates $\mathbf{r}$ between the two nucleons, and $\boldsymbol{\rho}$ between their center of mass (cm) and the core A. The core spin is I and the spin of the $A+2$ composite state is J. When intrinsic spins s_1, s_2 are also included in a particular coupling order such as $|\{L, (\ell, (s_1 s_2)S)j\}J_{12}, I; J\rangle$, we have the partial wave expansion

$$\phi_I^J(\mathbf{r}, \boldsymbol{\rho}) = \sum_{L\ell SjJ_{12}I} \phi_{I\mu_I}(\xi_c)\phi_{s_1}^{\sigma_1}\phi_{s_2}^{\sigma_2} Y_L^\Lambda(\hat{\mathbf{r}})Y_\ell^\mu(\hat{\boldsymbol{\rho}}) \frac{1}{r\rho} u_{12}(r,\rho)\langle J_{12}M_{12}I\mu_I|JM\rangle$$

$$\times \langle L\Lambda jm_{12}|J_{12}M_{12}\rangle\langle \ell\mu S\Sigma|jm_{12}\rangle\langle s_1\sigma_1 s_2\sigma_2|S\Sigma\rangle \,. \tag{1}$$

The radial wave function $u_{12}(r,\rho)$ can be given either as a cluster product of single-particle wave functions $u_{12}(r,\rho) = \Phi_L(r)\phi_\ell(\rho)$, input directly as a two-dimensional distribution e.g. from a Faddeev bound-state calculation, or calculated from the correlated sum of products of single-particle states with independent coordinates. These two-nucleon wave functions will in general be the eigenstates of a three-body bound state Schrödinger equation

$$[T_{\mathbf{r}} + T_{\boldsymbol{\rho}} + V_{1A} + V_{2A} + V_{12} - \varepsilon]\phi_I^J(\mathbf{r}, \boldsymbol{\rho}) = 0 \,, \tag{2}$$

where the V_{iA} are the potentials between nucleon i and the core, and V_{12} is the pairing interaction between the two nucleons.

Such two-particle states that come from shell-model calculations[22] or from Sturmian-basis calculations[23] are usually described by means of the $|\mathbf{r}_1, \mathbf{r}_2\rangle$ coordinates. This describes a pair state as

$$\varphi_{12}(\mathbf{r}_1, \mathbf{r}_2) = \sum_i c_i|(\ell_1(i), s_1)j_1(i), (\ell_2(i), s_2)j_2(i); J_{12}\rangle \tag{3}$$

The coefficients c_i for correlated basis states i and the single-particle wave functions $\varphi_{\ell s j}(\mathbf{r})$ contain all the physics information about the bound state needed to do a transfer calculation. Shell model codes[24] can produce the coefficients c_i needed here in terms of previously calculated eigenstates of the A and the $A+2$ systems. These states are then transformed into the centre-of-mass coordinates $|\mathbf{r}, \boldsymbol{\rho}\rangle$ of Eq. (1) using $\mathbf{r}_i = x_i \mathbf{r} + y_i \boldsymbol{\rho}$. For equal mass particles, $x_1 = x_2 = 1$, and $y_1 = -y_2 = \frac{1}{2}$.

The *vertex functions* of these bounds states are defined to be these bound state wave functions $\phi_I^J(\mathbf{r}, \boldsymbol{\rho})$ multiplied by the potentials which have zero effects after the transfer step is performed and all exit channel nuclei have completely separated. These potentials are therefore the sum V of the binding potentials $V_i^{\rm sp} = V_{\ell s j}(\mathbf{r}_i)$, namely $V = V_{1A}^{\rm sp} + V_{2B}^{\rm sp}$. (These are the individual potentials that should appear in the bound-state equation $[T_\mathbf{r} + V_{\ell s j}(\mathbf{r}) - \varepsilon]\varphi_{\ell s j}(\mathbf{r}) = 0$.) The vertex function does *not* include the nucleon–nucleon pair interaction $V_{12}(\mathbf{r}_1 - \mathbf{r}_2)$, since this potential produces binding effects in both the initial and final bound states. We denote by $V\phi_I^J(\mathbf{r}, \boldsymbol{\rho})$ the vertex function after transformation into Jacobi coordinates by the same method used to transform the wave function itself.

3. Post and Prior Coupling Forms of Transfer Matrix Elements

We now consider the Hamiltonian $\mathcal{H}$ for the whole system of $A + B + 2$ nucleons and described by system wave function Ψ for the complete transfer reaction $A(B + 2, B)A + 2$. Let the various $A + 2$ and $B + 2$ bound states be denoted by Φ_i for indices i. Then we may expand Ψ in terms of the Φ_i with some coefficients $\psi_i(\mathbf{R}_i)$ depending on the two-body separation vectors $\mathbf{R}_i$. This gives the channel expansion $\Psi = \sum_i \psi_i(\mathbf{R}_i)\Phi_i$.

The model Schrödinger's equation $[\mathcal{H} - E]\Psi = 0$ when projected separately onto the different basis states Φ_j, yields the set of equations

$$[E_j - H_j]\psi_j(\mathbf{R}_j) + \sum_{i \neq j}\langle\Phi_j|\mathcal{H} - E|\Phi_i\rangle\psi_i(\mathbf{R}_i) = 0\,, \qquad (4)$$

which couple together the unknown wave functions $\psi_i(\mathbf{R}_i)$. The channel Hamiltonians are defined by the diagonal $H_j - E_j = \langle\Phi_j|\mathcal{H} - E|\Phi_j\rangle$ such that the E_j are the asymptotic kinetic energies in channel j.

The off-diagonal matrix element $\langle\Phi_j|\mathcal{H} - E|\Phi_i\rangle$ has two different forms, depending on whether we expand

$$\mathcal{H} - E = H_j - E_j + V_j \text{ (the 'post' form)}$$

$$= H_i - E_i + V_i \text{ (the 'prior' form)}\,.$$

The name (post or prior) is determined by whether it is the initial or final channel whose Hamiltonian is used. The above Eq. (4), as written, has i as the initial

channel and j as the final channel for the indicated coupling. Thus

$$\langle \Phi_j | \mathcal{H} - E | \Phi_i \rangle = V_{ji}^{\text{post}} + [H_j - E_j] K_{ji} \quad \text{(post)} \tag{5}$$

$$\text{or} = V_{ji}^{\text{prior}} + K_{ji} [H_i - E_i] \quad \text{(prior)},$$

where

$$V_{ji}^{\text{post}} \equiv \langle \Phi_j | V_j | \Phi_i \rangle, \quad V_{ji}^{\text{prior}} \equiv \langle \Phi_j | V_i | \Phi_i \rangle, \quad K_{ji} \equiv \langle \Phi_j | \Phi_i \rangle. \tag{6}$$

The overlap function $K_{ji} = \langle \Phi_j | \Phi_i \rangle$ in Eqs. (5) and (6) arises from the non-orthogonality between the basis states Φ_i and Φ_j if these are in different mass partitions. The K_{ji} are non-local operators that go to zero asymptotically (R_i or $R_j \to \infty$). (Within the *same* partition, the Φ_i would be inelastic states, and would form an orthogonal set.)

The *first-order DWBA* matrix element use entrance ψ_i and exit ψ_j channel wave functions satisfying $[H_i - E_i]\psi_i = 0$ and $[H_j - E_j]\psi_j = 0$ respectively. Its matrix element is

$$T_{ji}^{(1)} = \langle \psi_j^{(-)} \Phi_j | \mathcal{H} - E | \Phi_i \psi_i^{(+)} \rangle. \tag{7}$$

The prior form of this is

$$\begin{aligned}
T_{ji}^{(\text{prior})} &= \langle \psi_j^{(-)} \Phi_j | H_i - E_i + V_i | \Phi_i \psi_i^{(+)} \rangle \\
&= \langle \psi_j^{(-)} \Phi_j | V_i | \Phi_i \psi_i^{(+)} \rangle + \langle \psi_j^{(-)} \Phi_j | \Phi_i [H_i - E_i] \psi_i^{(+)} \rangle \\
&= \langle \psi_j^{(-)} \Phi_j | V_i | \Phi_i \psi_i^{(+)} \rangle + 0 \\
&= \langle \psi_j^{(-)} | V_{ji}^{\text{prior}} | \psi_i^{(+)} \rangle.
\end{aligned} \tag{8}$$

Similarly, the equivalent post form is

$$\begin{aligned}
T_{ji}^{(\text{post})} &= \langle \psi_j^{(-)} \Phi_j | H_j - E_j + V_j | \Phi_i \psi_i^{(+)} \rangle \\
&= \langle \psi_j^{(-)} \Phi_j | V_i | \Phi_i \psi_i^{(+)} \rangle + \langle \psi_j^{(-)} [H_j - E_j] \Phi_j | \Phi_i \psi_i^{(+)} \rangle \\
&= \langle \psi_j^{(-)} \Phi_j | V_j | \Phi_i \psi_i^{(+)} \rangle + 0 \\
&= \langle \psi_j^{(-)} | V_{ji}^{\text{post}} | \psi_i^{(+)} \rangle.
\end{aligned} \tag{9}$$

Thus the non-orthogonality term disappears in first-order DWBA. Post and prior first-order DWBA matrix elements can be made to exactly agree numerically, if sufficient care is taken to ensure convergence of the non-local form factors.

Let a *second-order DWBA* matrix element use entrance channel i, exit channel k, and some intermediate channel j, as $i \to j \to k$. The propagation in the intermediate channel may be described in terms of the Green's function G_j, or equivalently within an iterated coupled-channels set. The two-step DWBA matrix element is

$$T_{ki}^{(2)} = \langle \psi_k^{(-)} | \langle \Phi_k | \mathcal{H} - E | \Phi_j \rangle G_j \langle \Phi_j | \mathcal{H} - E | \Phi_i \rangle | \psi_i^{(+)} \rangle. \tag{10}$$

Now there are *four* matrix elements that may be calculated, according to the first and the second Hamiltonian form chosen: post–post, post–prior, prior–post, and prior–prior. The terms prior and post for each step are used to refer to the initial or final channels *of that step*, not the overall incoming or outgoing channels. In 'prior–post', the prior refers to the first step, and the post refers to the second step.

The post–post form of this, for example, is

$$T_{ki}^{(\text{post,post})} = \langle \psi_k^{(-)}| \langle \Phi_k|H_k - E_k + V_k|\Phi_j\rangle G_j \langle \Phi_j|H_j - E_j + V_j|\Phi_i\rangle |\psi_i^{(+)}\rangle. \quad (11)$$

Here the $[H_k - E_k]$ can operate on the final ψ_k to give zero, but little can simplify the $[H_j - E_j]$ since $[H_j - E_j]G_j \neq 0$ always. Thus

$$\begin{aligned} T_{ki}^{(\text{post,post})} &= \langle \psi_k^{(-)}|V_{kj}^{\text{post}} G_j V_{ki}^{\text{post}}|\psi_i^{(+)}\rangle \\ &+ \langle \psi_k^{(-)}|V_{kj}^{\text{post}} G_j [H_j - E_j] K_{ji}|\psi_i^{(+)}\rangle. \end{aligned} \quad (12)$$

This second term is called a 'non-orthogonality term' since it involves the bound-state non-orthogonality overlaps $K_{ji} = \langle \Phi_j|\Phi_i\rangle$, which is significant when R_i and R_j are both within the range of the bound states.

Similar analyses for post–prior and prior–prior two-step DWBA expression also have non-orthogonality terms in the final form. The *prior–post form*, however, is

$$T_{ki}^{(\text{prior,post})} = \langle \psi_k^{(-)}| \langle \Phi_k|H_k - E_k + V_k|\Phi_j\rangle G_j \langle \Phi_j|H_i - E_i + V_i|\Phi_i\rangle |\psi_i^{(+)}\rangle. \quad (13)$$

Here the $[H_i - E_i]$ can also operate on the initial ψ_i to give zero, as well as $[H_k - E_k]$ on the ψ_k, so we have the simplest form

$$T_{ki}^{(\text{prior,post})} = \langle \psi_k^{(-)}|V_{kj}^{\text{post}} G_j V_{ji}^{\text{prior}}|\psi_i^{(+)}\rangle. \quad (14)$$

The non-orthogonality terms can thus be made to disappear in second-order DWBA if the first and second steps use the prior and post interactions respectively. If the non-orthogonality terms are included as necessary, the results should be the same whatever post or prior forms are used.

In third and higher-order transfer calculations, some non-orthogonality terms will always be present, but most pair transfer mechanisms can be well modeled as two-step processes.

4. Two-Nucleon Transfer Interaction

We now consider the specific transfer matrix element $V_{ji}^{\text{prior}} = \langle \Phi_j|V_i|\Phi_i\rangle$. Given an expression for this prior form, we may calculate the post interaction easily as $V_{ji}^{\text{post}} = (V_{ij}^{\text{prior}})^\dagger$. Take Φ_j to refer to the bound states of nucleus $A + 2$ outside core A, and Φ_i analogously for nucleus B.

The transfer interaction has therefore the nonlocal matrix element

$$\mathsf{V}_{ji}(\mathbf{R}_j, \mathbf{R}_i) = \langle \phi_{I_A}^{J_A}(\mathbf{r}, \boldsymbol{\rho}_A)|V_{1B}^{\text{sp}} + V_{2B}^{\text{sp}} + U_{AB} - U_i|\phi_{I_B}^{J_B}(\mathbf{r}, \boldsymbol{\rho}_B)\rangle. \quad (15)$$

As is usual in transfer operators, there are three kinds of potentials appearing here. First there are the binding potentials $V_{1B}^{\text{sp}}(\mathbf{r}_{1B}) + V_{2B}^{\text{sp}}(\mathbf{r}_{2B})$. Since these binding

potentials always appear while multiplied by their bound state wave functions, we need only store and use the vertex functions defined in Sec. 2. Secondly, there is the 'core–core' potential $U_{AB}(\mathbf{R}_{AB})$ between the core nuclei A and B. Finally is subtracted an optical potential. In this prior form we subtract the optical potential in the initial channel, $U_i(\mathbf{R}_i)$. The difference $U_{AB} - U_i$ of the two optical potentials is called the *remnant term*, and is sometimes taken to be small.

The integrals in Eq. (15) include integrating over the two-nucleon separation $\mathbf{r}$ as well as over their cm distance $\boldsymbol{\rho}_A$ from the core A. The $\mathbf{r}$ coordinate appears in both the initial and final states, and so is not labeled by A or B. This has the important consequence that neither the distance nor the angle of the $\mathbf{r}$ coordinate is changed in the transfer. Neither, therefore, is their relative angular momentum ℓ, and, for similar reasons, their spin couplings S and total angular momentum j. The two neutron transfer can hence be viewed as the transfer of a 'structured particle' $\{r, (\ell, (s_1 s_2)S)j\}$, and then becomes similar to the more familiar single-particle transfers. This means that when we also afterwards integrate over the coordinate $\boldsymbol{\rho}_A$, we can use the standard procedures already developed for one-particle transfer interactions.

5. Coordinate Transformations

The transfer mechanism requires the pair wave function to be expressed in the form of Eq. (1), so independent-particle forms of Eq. (3) have to be transformed in their coordinates as

$$\varphi_{12}(\mathbf{r}_1, \mathbf{r}_2) = \sum_u c_i \sum_{L\ell S j} |L, (\ell, (s_1 s_2)S)j; J_{12}T\rangle \phi_{L(\ell S)j}^{J_{12}T,i}(r, \rho). \tag{16}$$

A particular basis state i in the (r, ρ) coordinates is

$$\phi_{L(\ell S)j}^{J_{12},i}(r, \rho) = \langle L, (\ell, (s_1 s_2)S)j; J_{12}|(\ell_1(i), s_1)j_1(i), (\ell_2(i), s_2)j_2(i); J_{12}\rangle$$

$$\times \langle [Y_L(\hat{\mathbf{r}})Y_\ell(\hat{\rho})]_\lambda|[\varphi_{\ell_1 s_1 j_1}(\mathbf{r}_1)\varphi_{\ell_2 s_2 j_2}(\mathbf{r}_2)]_{J_{12}T}\rangle \tag{17}$$

where (suppressing the i indices for clarity), and including an isospin T to define the antisymmetrization,

$$\langle L, (\ell, (s_1 s_2)S)j; J_{12}T|(\ell_1, s_1)j_1, (\ell_2, s_2)j_2; J_{12}T\rangle$$

$$= \sum_\lambda \hat{\lambda}\hat{S}\hat{j_1}\hat{j_2} \begin{pmatrix} \ell_1 & \ell_2 & \lambda \\ s_1 & s_2 & S \\ j_1 & j_2 & J_{12} \end{pmatrix}$$

$$\times \frac{1 + (-1)^{\ell+S+T}}{\sqrt{2(1 + \delta_{\ell_1,\ell_2}\delta_{j_1,j_2})}} \hat{j}\hat{\lambda}W(L\ell J_{12}S; \lambda j)(-1)^{\ell+L-\lambda}. \tag{18}$$

The radial overlap integral can be derived by means of harmonic-oscillator expansions,[25] with the Bayman–Kallio expansion[26] or using the Moshinsky solid-harmonic

expansion.[27] This last method gives

$$K^\lambda_{\ell L:\ell_1\ell_2}(r,\rho) = \langle [Y_L(\hat{\mathbf{r}})Y_\ell(\hat{\boldsymbol{\rho}})]_\lambda | [\varphi_{\ell_1}(\mathbf{r}_1)\varphi_{\ell_2}(\mathbf{r}_2)]^\lambda \rangle \tag{19}$$

$$= \sum_{n_1 n_2} \binom{2\ell_1+1}{2n_1}^{\frac{1}{2}} \binom{2\ell_2+1}{2n_2}^{\frac{1}{2}} (x_1 r)^{\ell_1-n_1} (y_1\rho)^{n_1} (x_2 r)^{n_2} (y_2\rho)^{\ell_2-n_2}$$

$$\times \sum_Q \mathbf{q}^Q_{\ell_1\ell_2}(r,\rho)(2Q+1)\hat{\ell}_1\hat{\ell}_2\widehat{\ell_1-n_1}\widehat{\ell_2-n_2}\hat{L}\hat{\ell}$$

$$\times \sum_{\Lambda_1\Lambda_2} \begin{pmatrix} \ell_1-n_1 & n_2 & \Lambda_1 \\ 0 & 0 & 0 \end{pmatrix} \begin{pmatrix} \ell_w-n_2 & n_1 & \Lambda_2 \\ 0 & 0 & 0 \end{pmatrix}$$

$$\times \begin{pmatrix} \Lambda_1 & L & Q \\ 0 & 0 & 0 \end{pmatrix} \begin{pmatrix} \Lambda_2 & \ell & Q \\ 0 & 0 & 0 \end{pmatrix}$$

$$\times (-1)^{\ell_1+\ell_2+L+\Lambda_2}(2\Lambda_1+1)(2\Lambda_2+1)W(\Lambda_1 L\Lambda_2\ell; Q\lambda)$$

$$\times \begin{pmatrix} \ell_1-n_1 & n_2 & \Lambda_1 \\ n_1 & \ell_2-n_2 & \Lambda_2 \\ \ell_1 & \ell_2 & \lambda \end{pmatrix}, \tag{20}$$

where $\binom{a}{b}$ is a binomial coefficient. The kernel function $\mathbf{q}^Q_{\ell_1\ell_2}(r,\rho)$ is the Legendre expansion of the product of the two radial wave functions in terms of u, the cosine of the angle between $\mathbf{r}$ and $\boldsymbol{\rho}$:

$$\mathbf{q}^Q_{\ell_1,\ell_2}(r,\rho) = \frac{1}{2}\int_{-1}^{+1} \frac{\varphi_{\ell_1 s_1 j_1}(r_1)}{r_1}^{\ell_1+1} \frac{\varphi_{\ell_2 s_2 j_2}(r_2)}{r_2}^{\ell_2+1} P_Q(u)du. \tag{21}$$

6. Zero-Range and Other Approximations

The coupling potentials $\mathsf{V}_{ji}(\mathbf{R}_j, \mathbf{R}_i)$ of Eq. (15) are *nonlocal*, in the sense that in general the initial and final radii, $\mathbf{R}_j$ and $\mathbf{R}_i$, will be different. They will not only have different magnitudes, but also different directions. In the early days of transfer modeling, the calculations only became practical if a *zero-range* approximation could be found, in which the coupling was restricted to $\mathbf{R}_j = \alpha\mathbf{R}_i$ for some constant α (which need not be unity).

When the projectile is a light ion such as ^{3}H, ^{3}He or ^{4}He for nucleus $B+2$, then the binding potential sum $V^{\mathrm{sp}}_{1B} + V^{\mathrm{sp}}_{2B}$ will have short range. We may therefore consider approximating the vertex function

$$[V^{\mathrm{sp}}_{1B} + V^{\mathrm{sp}}_{2B}]\phi^{J_B}_{I_B}(\mathbf{r}, \boldsymbol{\rho}_B) \sim D_0\delta(\boldsymbol{\rho}_B)\phi^B_{nn}(\mathbf{r}) \tag{22}$$

for some nucleon–nucleon wave function $\phi_{nn}(\mathbf{r})$ that we are free to choose. This a zero-range approximation. Note that it is only $\boldsymbol{\rho}_B$ which needs to have zero range, not $\mathbf{r}$. The constant D_0 is called the *zero-range constant*.

If, furthermore, we can neglect the remnant term $U_{AB} - U_i$, then the transfer coupling of Eq. (15) can be simplified as

$$\mathsf{V}_{ji}(\mathbf{R}_j, \mathbf{R}_i) = \langle \phi_{I_A}^{J_A}(\mathbf{r}, \boldsymbol{\rho}_A)|V_{1B}^{\mathrm{sp}} + V_{2B}^{\mathrm{sp}}|\phi_{I_B}^{J_B}(\mathbf{r}, \boldsymbol{\rho}_B)\rangle$$

$$= \langle \phi_{I_A}^{J_A}(\mathbf{r}, \boldsymbol{\rho}_A)|D_0\delta(\boldsymbol{\rho}_B)\phi_{nn}^B(\mathbf{r})\rangle$$

$$= D_0\langle \phi_{nn}^B(\mathbf{r})|\phi_{I_A}^{J_A}(\mathbf{r}, \boldsymbol{\rho}_A)\rangle\delta(\boldsymbol{\rho}_B)$$

$$= D_0\langle \phi_{nn}^B(\mathbf{r})|\phi_{I_A}^{J_A}(\mathbf{r}, \boldsymbol{\rho}_A)\rangle\delta\left(\beta\left(\mathbf{R}_j - \frac{A}{A+2}\mathbf{R}_i\right)\right), \qquad (23)$$

since

$$\mathbf{R}_j - \frac{A}{A+2}\mathbf{R}_i = \boldsymbol{\rho}_B/\beta \quad \text{for} \quad \beta = \frac{2(A+B+2)}{(A+2)(B+2)}. \qquad (24)$$

That is, we arrive at a 'form factor' $\langle \phi_{nn}^B(\mathbf{r})|\phi_{I_A}^{J_A}(\mathbf{r}, -\mathbf{R}_j)\rangle$ that is local in $\mathbf{R}_j = \frac{A}{A+2}\mathbf{R}_i = -\boldsymbol{\rho}_A$ because of the delta function $\delta(\boldsymbol{\rho}_B)$. To find the form factor, we need to determine the average nucleon–nucleon relative wave function $\phi_{nn}^B(\mathbf{r})$ in the light ion, and project the heavy-nucleus two-body wave function $\phi_{I_A}^{J_A}(\mathbf{r}, \boldsymbol{\rho}_A)$ onto this relative motion. This gives a function only of the distance $\rho_A = R_j$ and the angles. The kinematics for this zero-range approximation are identical to those for the one-body transfer of a mass-2 cluster from core B to core A. A local-energy approximation may be used to improve the treatment of the finite range of the vertex function, just as for one-body transfers.

This is a further example the conclusion stated at the end of Sec. 4, namely that transfer reactions only probe in the unknown nucleus those components of nn relative motion that already exist in the known nucleus. Since the known light nuclei ^{3}H, ^{3}He and ^{4}He have predominantly s-wave relative motion between the two transferred nucleons, our transfer reactions will only probe pairing states of s-wave relative motion in the target. The *magnitude* of the transfer cross section will be proportional to the form factor overlap $\langle \phi_{nn}^B(\mathbf{r})|\phi_{I_A}^{J_A}(\mathbf{r}, \boldsymbol{\rho}_A)\rangle$.

Zero-range approximations can be also used for some of the sequential steps involving these light nuclei, but not for all of them if we are using 'prior–post' couplings to avoid non-orthogonality corrections. For stripping reactions such as (t,p), the first prior (t,d) step has no good zero-range approximation, and for pickup reactions such as (p,t), the second post (d,t) step must be treated in full finite range for the same reason.

7. Results

In this short paper we will focus on the reaction mechanisms for the pair transfer ^{124}Sn(p,t)^{122}Sn at 25 MeV, using the overlap function shown in Table 1 we find by overlapping the shell-model wave functions for the ground states of ^{122}Sn and ^{124}Sn. The structure results for ^{124}Sn and ^{122}Sn were obtained in the model space

Table 1.   Two-neutron overlap
function for $\langle {}^{122}\mathrm{Sn}|{}^{124}\mathrm{Sn}\rangle$.

$1g_{7/2}^2$	0.62944
$2d_{5/2}^2$	0.59927
$2d_{3/2}^2$	0.71913
$3s_{1/2}^2$	0.51892
$1h_{11/2}^2$	−1.24399

of $(0g_{7/2}, 1d_{5/2}, 1d_{3/2}, 2s_{1/2}, 0h_{11/2})$ for neutrons with the code NuShell.[24] The model-space two-body matrix elements are those used in Refs. 29 and 30. They were obtained starting with a G matrix derived from the CD–Bonn[31] nucleon–nucleon interaction. The harmonic oscillator basis was employed for the radial wave functions with an oscillator energy $\hbar\omega = 7.87$ MeV. The effective interaction for the above shell-model space is obtained from the Q-box method and includes all non-folded diagrams through third-order in the interaction G to sum up the folded diagrams to infinite order.[32,33] The single-particle energies were adjusted to reproduce the observed states in ${}^{131}\mathrm{Sn}$.

The inputs to the reaction code are the two-nucleon spectroscopic amplitudes (TNA) of Table 1. A center of mass correction[34] equal to $[A/(A-2)]^{2n+\ell}$ for the TNA has been applied, where $A = 124$. Our sign convention is that the radial wave functions are positive at the origin. The sequential process was calculated by a single intermediate state for each of these orbits connected by a product of one-nucleon spectroscopic amplitudes that are equal to the center-of-mass corrected TNA multiplied by $\sqrt{2}$ that takes into account the normalization of the two-particle amplitude. Future calculations should also take into account the TNA obtained from the mixing of neutron pairs for orbitals outside of the model space.

We use the triton potential of Li,[35] the deuteron potential of Daehnick,[36] and the proton potential of Chapel Hill 89.[37] All the two-neutron wave functions are constructed within the half-separation-energy prescription. For a triton wave function we use the pure s^2 configuration found by the product of eigenstates at the half-separation energy (4.24 MeV) in a Woods–Saxon potential with $V = 77.83$ MeV, $R = 0.95$ fm, and $a = 0.65$ fm (the results are not sensitive to these values). The Sn wave functions shown in Table 1 are found at the half-separation energy (7.219 MeV) in a WS potential with $r = 1.17$ fm, and $a = 0.75$ fm that has the fixed spin-orbit component $V_{so} = 6.2$ MeV, $r = 1.01$ fm, and $a = 0.75$ fm.

The complete cross section prediction is shown in Fig. 1, compared with the experimental data of Guazzoni *et al.*[28] Now we see that, with the shell-model overlaps and proper finite-range and sequential contributions, the unhappiness factors are much closer to unity. A better agreement between theory and experiment has already been published,[19] but in the present calculations there are still questions about the angular oscillations which are in not so good agreement with experiment. Note that Guazzoni *et al.*[28] took the better agreement of the *simultaneous* transfer
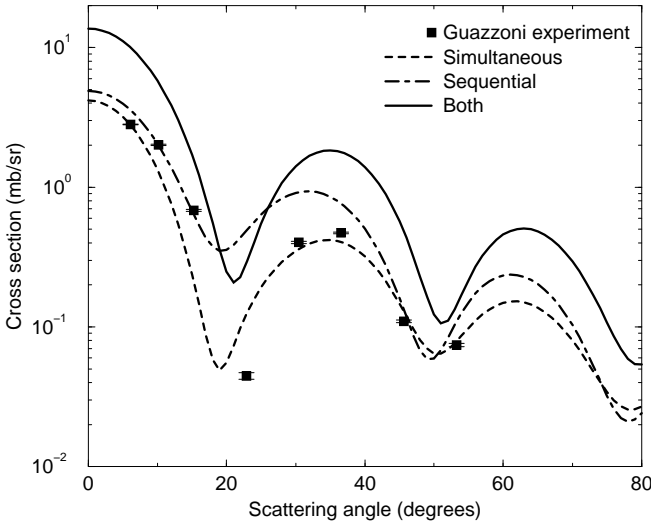
Fig. 1.   Simultaneous (short dash), sequential (dot-dash) and simultaneous + sequential (solid line) cross sections for the reaction ^{124}Sn(p,t)^{122}Sn at 25 MeV, in comparison with the experimental data of Guazzoni *et al.*[28]

curve (dashed line) to indicate small effects for sequential transfers, but this is not correct since we do know that sequential transfers occur, and can calculate them with good accuracy in this model (dot-dashed line).

To see the importance of the nonorthogonality terms, and hence of choosing 'prior–post' couplings if nonorthogonality terms are to be avoided, Fig. 2 plots the different sequential cross sections for all possible combinations of post and prior for the two steps. The prior–post solid curve is the dot-dashed curve in Fig. 1. The other curves are all different from this one, and cannot be simply added to the simultaneous amplitude to get the correct result. This also implies that no complete calculation with only zero-range couplings is possible.

Finally, it is instructive to look at the interference effects between the various simultaneous and sequential contributions. To display these coherence effects, I choose to plot the scattering amplitude at zero degrees for the non-spin-flip amplitude $m_p = m_t = 1/2$ (the only nonzero amplitude at this angle). Figure 3 plots all the simultaneous and sequential contributions from the different components listed in Table 1, along with their coherent sums. We see that all the contributions to the simultaneous transfer are constructively coherent, as are all the contributions to the total sequential amplitude. This constructive coherence follows from the signs of the amplitudes in Table 1, and reflects the significant pairing enhancement in ^{124}Sn. The total sequential and simultaneous amplitudes are not uniformly coherent with each other, however. A uniform 90° angle between the simultaneous and sequential amplitudes in Fig. 3 would indicate an incoherent summation of the two
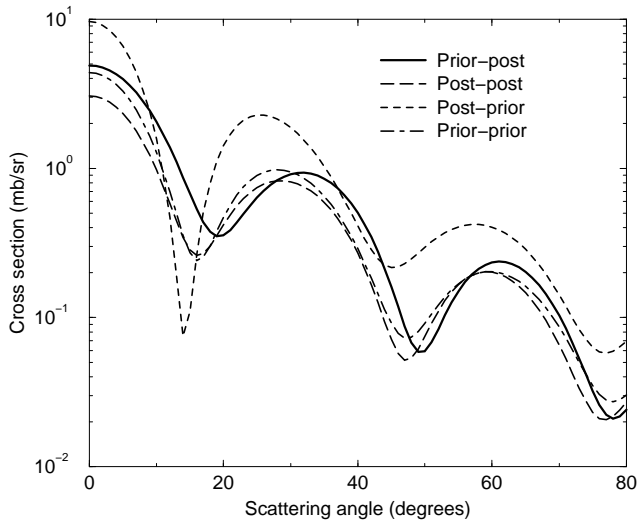
Fig. 2.   Sequential cross sections for all possible combinations of post and prior for the two steps.
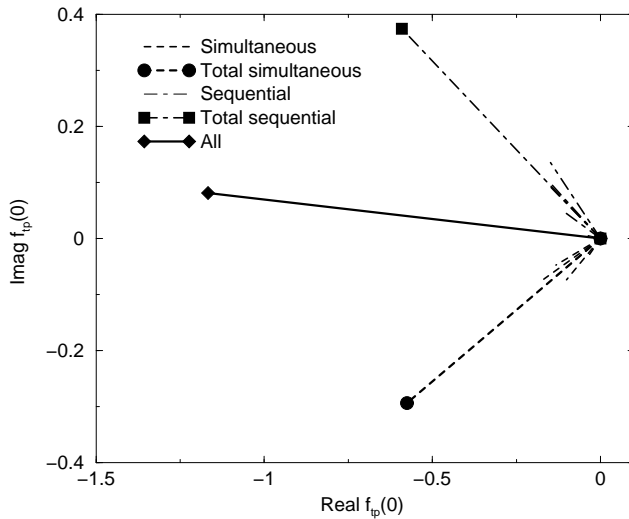

Fig. 3.   Simultaneous (short dash), sequential (dot-dash) and simultaneous+sequential (solid line) amplitudes at zero degrees for the reaction ^{124}Sn(p,t)^{122}Sn at 25 MeV. The short lines show the individual contributions from the wave function components of Table 1, and the longer lines with symbols are their coherent sums.

cross sections, but that is not exactly true either. This reflects the importance of the deuteron channel with its own specific optical potential. In general, varying deuteron optical potentials and differing intermediate Q-values require that both simultaneous and sequential terms be explicitly calculated.

Acknowledgements

References

1. S. Yoshida, Note on the two-nucleon stripping reaction, *Nuclear Physics* **33**, 685–692 (1962).
2. N. K. Glendenning, Nuclear spectroscopy with two-nucleon transfer reactions, *Phys. Rev.* **137**, B102–B113 (Jan, 1965).
3. J. Bjerregaard, O. Hansen, O. Nathan and S. Hinds, The (t,p) reaction with the even isotopes of sm, *Nuclear Physics* **86**(1), 145–166 (1966).
4. R. J. Ascuitto and N. K. Glendenning, Inelastic processes in particle transfer reactions, *Phys. Rev.* **181**, 1396–1403 (May, 1969).
5. R. Ascuitto, N. Glendenning and B. Srensen, Confirmation of strong second order processes in (p,t) reactions on deformed nuclei, *Phys. Lett. B* **34**(1), 17–20 (1971).
6. B. Bayman, Finite-range calculation of the two-neutron transfer reaction, *Nuclear Physics A* **168**(1), 1–16 (1971).
7. R. Broglia, The pairing model, *Annals of Physics* **80**(1), 60–85 (1973).
8. L. A. Charlton, Finite-range evaluation of $(p\text{-}d,d\text{-}t)$ with momentum space techniques, *Phys. Rev. C* **14**, 506–513 (Aug, 1976).
9. M. Yasue, H. Yokomizo, S. Kubono, K. Koyama, S. Takeuchi and H. Ohnuma, ^{12}C(p,t)^{10}C and ^{12}C(p,^{3}He)^{10}B Reactions at Ep = 51.9 MeV, *Journal of the Physical Society of Japan* **42**, 367 (1977).
10. N. Hashimoto and M. Kawai, The (p,d) (d,t) process in strong (p,t) reactions, *Progress of Theoretical Physics* **59**(4), 1245–1260 (1978).
11. T. Takemasa, T. Tamura and T. Udagawa, Exact finite range calculations of light-ion induced two-neutron transfer reactions, *Nuclear Physics A* **321**(2), 269–294 (1979).
12. B. F. Bayman and J. Chen, One-step and two-step contributions to two-nucleon transfer reactions, *Phys. Rev. C* **26**, 1509–1520 (Oct, 1982).
13. E. Maglione, G. Pollarolo, A. Vitturi, R. Broglia and A. Winther, Absolute cross sections of two-nucleon transfer reactions induced by heavy ions, *Phys. Lett. B* **162**(13), 59–65 (1985).
14. M. Kurokawa, Y. Aoki, Y. Tagishi and K. Yagi, One-and two-step processes in natural-and unnatural-parity ^{208}Pb(p,t)^{206}Pb reaction at $E_p = 22$ MeV, *Nucl. Phys. A* **470**(2), 377–396 (1987).
15. M. Igarashi, K. Kubo and K. Yagi, Two-nucleon transfer reaction mechanisms, *Physics Reports* **199**(1), 1–72 (1991).
16. I. Tanihata, M. Alcorta, D. Bandyopadhyay, R. Bieri, L. Buchmann, B. Davids, N. Galinski, D. Howell, W. Mills, S. Mythili, R. Openshaw, E. Padilla-Rodal, G. Ruprecht, G. Sheffer, A. C. Shotter, M. Trinczek, P. Walden, H. Savajols, T. Roger, M. Caamano, W. Mittig, P. Roussel-Chomaz, R. Kanungo, A. Gallant, M. Notani, G. Savard and I. J. Thompson, Measurement of the two-halo neutron transfer reaction ^{1}H(^{11}Li,^{9}Li)^{3}H at 3A MeV, *Phys. Rev. Lett.* **100**, 192502 (May, 2008).
17. G. Potel, A. Idini, F. Barranco, E. Vigezzi and R. A. Broglia, Single cooper pair transfer in stable and in exotic nuclei, *arXiv/0906.4298v3.* **nucl-th** (April, 2011).

18. G. Potel, F. Barranco, E. Vigezzi and R. A. Broglia, Evidence for phonon mediated pairing interaction in the halo of the nucleus ^{11}Li, *Phys. Rev. Lett.* **105**, 172502 (Oct, 2010).

19. G. Potel, F. Barranco, F. Marini, A. Idini, E. Vigezzi and R. A. Broglia, Calculation of the transition from pairing vibrational to pairing rotational regimes between magic nuclei ^{100}Sn and ^{132}Sn via two-nucleon transfer reactions, *Phys. Rev. Lett.* **107**, 092501 (Aug, 2011).

20. M. C. Mermaz, A. Greiner, B. T. Kim, M. A. G. Fernandes, N. Lisbona, E. Müller, W. Chung and B. H. Wildenthal, Multinucleon transfer reactions induced by ^{18}O on ^{28}Si, *Phys. Rev. C* **20**, 2130–2142 (Dec, 1979).

21. J. S. Vaagen and K. Kumar, Matrix elements for scattering and two-nucleon transfer operators derived from dynamic deformation theory wavefunctions, *Journal of Physics G: Nuclear Physics* **5**(9), 1211 (1979).

22. S. Cohen and D. Kurath, Two-nucleon transfer in the 1p shell, *Nucl. Phys. A* **141**(1), 145–157 (1970).

23. J. Bang, F. Gareev, W. Pinkston and J. S. Vaagen, One- and two-nucleon overlap functions in nuclear physics, *Phys. Rep.* **125**(6), 253–399 (1985).

24. B. A. Brown and W. D. M. Rae, Nushell@MSU. MSU-NSCL report, (2007).

25. T. Brody and M. Moshinsky, *Tables of Transformation Brackets* (Monografias del Instituto de Fisica, 1960).

26. B. F. Bayman and A. Kallio, Relative-angular-momentum-zero part of two-nucleon wave functions, *Phys. Rev.* **156**, 1121–1128 (Apr, 1967).

27. M. Moshinsky, Transformation brackets for harmonic oscillator functions, *Nuclear Physics* **13**(1), 104–116 (1959).

28. P. Guazzoni, L. Zetta, A. Covello, A. Gargano, B. Bayman, T. Faestermann, G. Graw, R. Hertenberger, H.-F. Wirth and M. Jaskola, High-resolution measurement of the ^{118,124}Sn(p,t)^{116,122}Sn reactions: Shell-model and microscopic distorted-wave Born approximation calculations, *Phys. Rev. C* **83**(4), 044614 (Apr, 2011).

29. B. A. Brown, N. J. Stone, J. R. Stone, I. S. Towner and M. Hjorth-Jensen, Magnetic moments of the 2_1^+ states around ^{132}Sn, *Phys. Rev. C* **71**, 044317 (Apr, 2005).

30. B. A. Brown, N. J. Stone, J. R. Stone, I. S. Towner and M. Hjorth-Jensen, Erratum: Magnetic moments of the 2_1^+ states around ^{132}Sn, *Phys. Rev. C* **72**, 029901 (Aug, 2005).

31. R. Machleidt, F. Sammarruca and Y. Song, Nonlocal nature of the nuclear force and its impact on nuclear structure, *Phys. Rev. C* **53**, R1483–R1487 (Apr, 1996).

32. M. Hjorth-Jensen, T. T. Kuo and E. Osnes, Realistic effective interactions for nuclear systems, *Physics Reports* **261**(34), 125–270 (1995).

33. M. Hjorth-Jensen, H. Müther, E. Osnes and A. Polls, Comparison of the effective interaction to various orders in different mass regions, *Journal of Physics G: Nuclear and Particle Physics* **22**(3), 321 (1996).

34. N. Anyas-Weiss, J. Cornell, P. Fisher, P. Hudson, A. Menchaca-Rocha, D. Millener, A. Panagiotou, D. Scott, D. Strottman, D. Brink, B. Buck, P. Ellis, and T. Engeland, Nuclear structure of light nuclei using the selectivity of high energy transfer reactions with heavy ions, *Physics Reports* **12**(3), 201–272 (1974).

35. X. Li, C. Liang and C. Cai, Global triton optical model potential, *Nuclear Physics A* **789**(14), 103–113 (2007).

36. W. W. Daehnick, J. D. Childs and Z. Vrcelj, Global optical model potential for elastic deuteron scattering from 12 to 90 MeV, *Phys. Rev. C* **21**, 2253–2274 (Jun, 1980).

37. R. Varner, W. Thompson, T. McAbee, E. Ludwig and T. Clegg, A global nucleon optical model potential, *Physics Reports* **201**(2), 57–119 (1991).